

See discussions, stats, and author profiles for this publication at: <https://www.researchgate.net/publication/14254027>

# Membrane-Binding and Lipid Vesicle Cross-Linking Kinetics of the Mitochondrial Creatine Kinase Octamer

ARTICLE *in* BIOCHEMISTRY · JANUARY 1997

Impact Factor: 3.02 · DOI: 10.1021/bi961838v · Source: PubMed

---

CITATIONS

41

---

READS

16

3 AUTHORS, INCLUDING:



Theo Wallimann

ETH Zurich

287 PUBLICATIONS 15,202 CITATIONS

SEE PROFILE

# Membrane-Binding and Lipid Vesicle Cross-Linking Kinetics of the Mitochondrial Creatine Kinase Octamer<sup>†</sup>

Olaf Stachowiak,\* Max Dolder, and Theo Wallimann

*Institute for Cell Biology, Swiss Federal Institute of Technology, ETH-Hönggerberg, CH-8093 Zürich, Switzerland*

*Received July 24, 1996; Revised Manuscript Received September 26, 1996<sup>®</sup>*

**ABSTRACT:** Mitochondrial creatine kinase (Mi-CK; EC 2.7.3.2) is a positively charged enzyme located between the mitochondrial inner and outer membrane as well as along the cristae membranes. The octameric form of Mi-CK is able to cross-link membranes to form contact sites. The process of Mi-CK membrane binding and Mi-CK-induced cross-linking of model membrane vesicles containing different amounts of cardiolipin (CL) was investigated *in vitro*. First, the direct binding of octameric Mi-CK to immobilized lipid vesicles containing cardiolipin was monitored by plasmon resonance (BiaCore). The analysis of the pseudo-first-order on- and off-rate constants indicates that there are two binding sites with different affinity for Mi-CK on the membrane. The association equilibrium constants obtained at 25 °C were 813.7 (for 100% CL) and 343.6 (for 16% CL), respectively, for the high-affinity binding mode. Second, the Mi-CK-induced vesicle cross-linking kinetics were analyzed by fixed-angle light scattering. Only octameric Mi-CK induced bridged vesicle/protein complexes, whereas dimeric Mi-CK failed to induce vesicle cross-linking. For vesicles containing 100% cardiolipin, the pseudo-first-order association rate constant was  $2.55 \times 10^{-3} \text{ s}^{-1}$ , while for membranes containing 16% cardiolipin and 84% PC a constant of  $6.25 \times 10^{-3} \text{ s}^{-1}$  was found. The examined kinetic properties of the system suggest a two-step model for Mi-CK-induced vesicle cross-linking which consists of a fast binding step of the enzyme to the membrane, followed by a remarkably slower cross-linking reaction between Mi-CK-covered vesicles. The data obtained by *in vitro* biophysical methods agree with earlier experiments done with mitoplasts and isolated mitochondrial membranes and explain the *in vivo* accumulation of Mi-CK at contact sites between the inner and outer mitochondrial membrane and the formation of Mi-CK-rich intramitochondrial inclusions observed in creatine-depleted animals as well as in patients with mitochondrial cytopathies.

Creatine kinase (CK)<sup>1</sup> is a key enzyme of energy metabolism which catalyzes the reversible transfer of a phosphoryl group from phosphocreatine (PCr) to ADP, thereby replenishing the ATP pool of the cell. CK plays an important role in tissues that have a high and fluctuating energy demand like muscle or brain and is often attached to subcellular structures. For example, in muscle, some CK is specifically bound to the myofibrillar M-band, the sarcoplasmic reticulum, and the mitochondria where the enzyme is functionally coupled to the actomyosin ATPase, the  $\text{Ca}^{2+}$ -ATPase, the  $\text{Na}^+/\text{K}^+$ -ATPase, and oxidative phosphorylation, respectively (for review see Wallimann et al., 1992, and Wallimann, 1994). There are different isoforms of CK which are distributed in a tissue- and compartment-specific manner (for review see: Eppenberger et al., 1983; Wallimann et al., 1992; Wyss et al., 1992 and references therein). The cytosolic isoforms are always homo- or heterodimeric (MM-, MB-, or BB-CK), whereas the mitochondrial isoforms of CK also

form octamers. Mi-CKs are localized between the inner and outer mitochondrial membrane where they are bound to the cardiolipin-rich inner leaflet (Müller et al., 1985) and along the cristae membranes (Wegmann, 1991). The octamer consists of four homodimers ( $M_r(\text{dimer}) = 84\,000$ ) displaying a  $P422$  symmetry which gives rise to a cube-shaped molecule (Schnyder et al., 1991). The high-resolution crystal structure of octameric  $\text{Mi}_b\text{-CK}$  which has recently been determined (Fritz-Wolf et al., 1996) shows that the four banana-shaped dimers are arranged in a tilted manner exhibiting four lysine-rich C-termini at the top and another four at the bottom face of the octamer. This arrangement is very likely to be responsible for membrane binding and vesicle cross-linking by noncovalent interactions. The high affinity of octameric Mi-CK for the mitochondrial inner membrane has been shown qualitatively for mitoplasts (Lipskaya & Trofimova, 1989b; Marcillat et al., 1987; Vial et al., 1979), leading to the conclusion that there are two different binding sites for octameric Mi-CK on the inner mitochondrial membrane (Schlame & Augustin, 1985). Experiments with isolated mitochondrial membranes have shown the possibility of generating Mi-CK-induced inter-cristae contacts as well as contacts between both membranes (Rojo et al., 1991a,b). Evidence for a key role of Mi-CK in mitochondrial membrane contact sites *in vivo* has been put forward as well (Brdiczka, 1991; Kottke et al., 1991). In addition, it has been shown that Mi-CK is able to interact with porin of the outer mitochondrial membrane (Brdiczka et al., 1994)

<sup>†</sup> This work was supported by an ETH graduate-student grant (for O.S.), by the Swiss National Science Foundation (Grant 31-33907.92 to T.W.), and by private sponsoring (Cereal Holding, Zürich, for M.D.).

\* To whom correspondence should be addressed. Tel: +41-6333339; Fax: +41-1-6331069; E-mail: stachowi@cell.biol.ethz.ch.

<sup>®</sup> Abstract published in *Advance ACS Abstracts*, November 1, 1996.

<sup>1</sup> Abbreviations: ANT, adenine nucleotide translocase; Biotin-X-DHPE, *N*-(6-(biotinoylamino)hexanoyl)-1,2-dihexadecanoyl-*sn*-glycero-3-phosphoethanolamine; CK, creatine kinase; CL, cardiolipin; 2-ME, 2-mercaptoethanol;  $\text{Mi}_b\text{-CK}$ , chicken sarcomeric muscle mitochondrial creatine kinase; PC, phosphatidylcholine; TES, *N*-[tris(hydroxymethyl)methyl]-2-aminoethanesulfonic acid; TSAC, transition-state analog complex.

whereas cardiolipin (CL) has been identified as one possible inner-membrane receptor of Mi-CK (Müller et al., 1985). A functional coupling of Mi-CK to the adenine nucleotide translocase (ANT; synonyms: AAC, ADT1) has been demonstrated experimentally with isolated mitochondria and permeabilized cells (Jacobus, 1985; Saks et al., 1985, 1994), indicating that Mi-CK has preferential access to mitochondrial matrix-produced ATP transported by the ANT. Therefore, it has been proposed that the ANT which is associated with several tightly bound cardiolipin molecules (Beyer & Klingenberg, 1985) may also be a possible receptor for Mi-CK in the inner membrane. Thus, a complex of porin, ANT, and Mi-CK may play an important role in mitochondrial "metabolic channeling" where the production of ATP is combined with its transphosphorylation to PCr by Mi-CK and the translocation of the latter through the outer mitochondrial membrane into the cytosol (Brdiczka, 1991; Wallimann et al., 1992; Wyss & Wallimann, 1992; Wallimann, 1994).

So far, no quantitative data on the Mi-CK membrane-binding and cross-linking kinetics have been published. In this work, we have investigated the binding of Mi-CK to model membranes by plasmon resonance using immobilized vesicles. From these measurements, the kinetics of Mi-CK binding and dissociation could be directly deduced. In addition, the kinetics of Mi-CK-induced vesicle cross-linking was analyzed by light scattering. The data obtained in the present study will contribute to the understanding of Mi-CK/membrane interactions and provide the basis for a quantitative treatment of Mi-CK binding to reconstituted membrane proteins.

## MATERIALS AND METHODS

**Overexpression and Isolation of *Mi<sub>b</sub>*-CK.** Chicken sarcomeric mitochondrial creatine kinase (*Mi<sub>b</sub>*-CK) was produced by overexpression of the pRF23 vector in the *Escherichia coli* strain BL21(DE3)pLysS. The protein was purified by a combination of Blue Sepharose affinity chromatography and cation exchange chromatography on a Mono S HR5/5 FPLC column (Pharmacia) as described (Furter et al., 1992). Concentrated *Mi<sub>b</sub>*-CK (5 mg/mL) was stored in Mono S elution buffer at  $-80^{\circ}\text{C}$ . Kinase activity was measured by the pH-stat assay (Wallimann et al., 1984) determining the rate of ATP formation (reverse reaction). Dimeric *Mi<sub>b</sub>*-CK was produced by incubating octameric CK in TSAC mixture (transition-state analog complex) for 24 h (Gross & Wallimann, 1993). Protein concentration was determined using the Bio-Rad assay (Bradford, 1976) using BSA as standard.

**Production of Large Unilamellar Vesicles (LUVETS).** Vesicles were produced using a combination of the freeze/thawing technique and the extrusion technique (MacDonald et al., 1990). Briefly, lipids (purchased from Sigma (cardiolipin) and Lipid Products (egg yolk PC)) in chloroform/methanol (2:1) solution were dried in a round bottom flask attached to a rotary evaporator. To achieve complete dryness, flasks were connected to a vacuum trap for several hours. The lipid film was resuspended in buffer (10 mM TES, 50 mM NaCl, pH 7.0) using glass beads to remove the film from the glass wall. The crude lipid suspension was freeze/thawed 15 times using liquid nitrogen as freezing agent and a water bath ( $30^{\circ}\text{C}$ ) for thawing. Then the

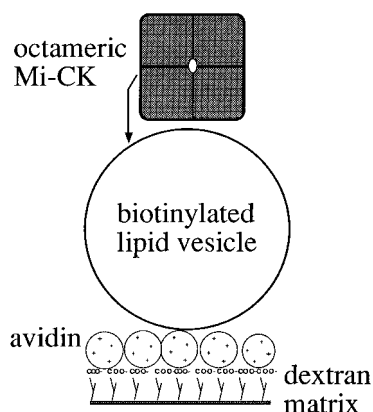


FIGURE 1: Schematic view of the sensor chip surface used in the BiaCore. The surface created to measure the association of octameric *Mi-CK* to immobilized vesicles consists of an avidin layer coupled to a CM5 sensor chip. Biotinylated vesicles are then immobilized on this surface before *Mi-CK* is injected and its binding monitored in real time by the increase of the response signal. Injection of running buffer at the end of the association of *Mi-CK* delivers the information for the dissociation phase.

suspension was passed 20 times through a polycarbonate membrane (Avestin) with a pore diameter of 200 nm mounted in a Mini-Extruder (Avestin) to form unilamellar liposomes with a diameter of about 160 nm. Vesicles thus formed were routinely checked by electron microscopy. Lipid concentration was measured using a modified Fiske/Subbarow method (Bartlett, 1959). For the BiaCore measurements 0.1% (w/w) Biotin-X-DHPE (Molecular Probes) was added to the lipid solution before drying it.

**Plasmon Resonance (BiaCore).** Plasmon resonance was measured at  $25^{\circ}\text{C}$  using real-time BIA (biomolecular interaction analysis) in a BiaCore instrument (Biosensor). A stable surface with avidin-immobilized biotinylated liposomes was created according to the method described by Masson and co-workers (Masson et al., 1994). Avidin was immobilized on a CM5 carboxymethyl sensor chip using routine amine coupling chemistry with *N*-hydroxysuccinimide (NHS) and *N*-ethyl-*N'*-((dimethylamino)propyl)carbodiimide (EDC) (Johnsson et al., 1991). Vesicles (16% cardiolipin, 83.9% PC, 0.1% Biotin-X-DHPE (Molecular Probes), or 99.9% cardiolipin, 0.1% Biotin-X-DHPE) were diluted in TES/NaCl buffer to a lipid concentration of 0.05 mg/mL and injected into the system to achieve a final signal increase of 600–1200 RU (response units). *Mi<sub>b</sub>*-CK stock solution was injected at different concentrations (0.17–1.36  $\mu\text{M}$ ) in running buffer (10 mM TES, 50 mM NaCl, pH 7.0). For all experiments the flow rate was set to 0.3 mL/h. Several series of measurements were performed in programmed cycles which consisted of vesicle immobilization, *Mi-CK* binding, and *Mi-CK* dissociation. To allow the proper determination of each rate constant, the results of 12 measurements at different *Mi-CK* concentrations were averaged. After each cycle, the avidin layer on the chip was washed with 1% SDS solution to remove bound liposomes and the protein. At the beginning of each new cycle 300–1200 RU of vesicles were rebound to the avidin surface to have reproducible binding and dissociation conditions for creatine kinase (see Figure 1 for schematic assay setup).

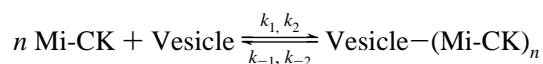
**Static Light Scattering.** Light scattering was measured at an angle of  $90^{\circ}$  using a SPEX fluorolog-2 instrument with a 450 W xenon arc lamp as light source. Intensity was measured using a single photon counter equipped with a

Peltier cooling unit. Excitation and detection wavelength was 420 nm. The excitation slit width was set to 0.2 nm, the emission slit width to 2 nm. All measurements were carried out at 25 °C in a stirred 1-cm quartz cuvette put into a thermostated sample holder. The reaction buffer was 10 mM TES/50 mM NaCl/2 mM 2-ME. Cuvettes were coated with 50 mM poly(L-lysine) (average MW 200 kDa, Sigma) and washed with buffer several times to minimize unspecific enzyme adsorption to the cuvette walls. Vesicles were preincubated for 45 min in buffer to achieve a constant scattering signal. Measurements were started by addition of the proper Mi-CK dilution in buffer.

## RESULTS

**Association/Dissociation Kinetics of Mi-CK to Immobilized Vesicles.** The direct reaction of Mi-CK with PC/CL vesicles was measured in a BiaCore system (Figure 1). This technique using avidin-immobilized biotinylated vesicles was chosen as there is immediate cross-linking of vesicles induced by octameric Mi-CK in free solution (see below). Avidin, like Mi-CK, has a high *pI*. Therefore, nonspecific binding of Mi-CK could be neglected as was tested by injecting Mi-CK onto the avidin surface lacking the vesicles. In addition, the immobilized avidin is not significantly affected by several washes with 1% SDS which was most efficient to regenerate the avidin surface for each new cycle of measurement. Therefore, several measurement cycles can be run with a constant amount of vesicles being immobilized before each Mi-CK injection. Other methods to remove bound Mi-CK like the use of high phosphate buffers lead to incomplete release of the protein and, consequently, to the accumulation of residual Mi-CK after each cycle which falsified the association measurements.

To see the effect of different CL contents on the Mi-CK membrane-binding behavior, two different kinds of liposomes were prepared, containing either 16% CL and 84% PC, or 100% CL. Figure 2 shows an association/dissociation cycle of Mi-CK and immobilized vesicles measured in the BiaCore for two sets of experimental conditions. The response signal is proportional to the amount of Mi-CK bound to vesicles at each time point. Irrespective of the lipid composition of the vesicles, the best fit for both the association and dissociation reaction turned out to be a sum of two exponential functions according to the following scheme:



This model implies that there are two independent binding sites for Mi-CK on the immobilized vesicles with different affinities as has been proposed for mitoplasts (Lipskaya & Trofimova, 1989a,b; Schlame & Augustin, 1985), leading to two simultaneously occurring association and dissociation reactions. The measured time courses were fitted on an Apple Macintosh system using the Kaleidagraph data evaluation program. The fit function for the association was

$$y = m_1 - ((m_1 - m_2)e^{-k_1 t} + m_2 e^{-k_2 t}) \quad (1)$$

where *y* represents the response signal, *m*<sub>1</sub> the estimated asymptotic value of the response signal (response units, RU), *m*<sub>2</sub> the amplitude associated with the second exponential term

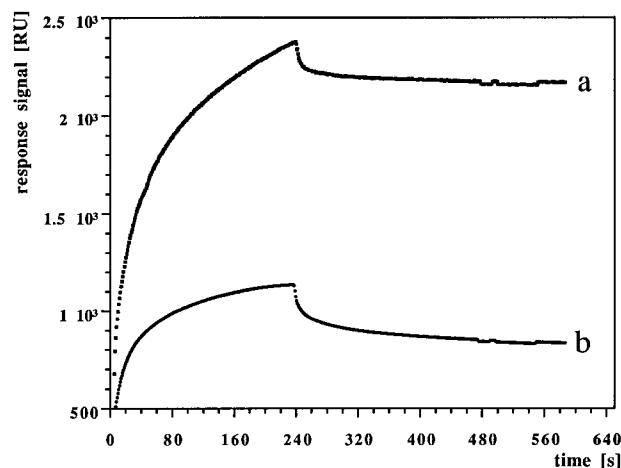


FIGURE 2: Association and dissociation kinetics of octameric Mi-CK and immobilized vesicles. The CM5 sensor chip was covered with 16 000 RU of avidin. Vesicles (5  $\mu$ L, lipid concentration 0.05 mg/mL) were then immobilized to give a response signal of 600 RU. Octameric Mi-CK was injected at a flow rate of 0.3 mL/h. The upper time course (a) shows the association phase (0–240 s) and the dissociation phase (240–580 s) of 20  $\mu$ L octameric Mi-CK solution ( $1.36 \times 10^{-6}$  M) reacting with surface-bound vesicles containing 100% CL. The lower time course (b) displays 20  $\mu$ L of  $6.8 \times 10^{-7}$  M octameric Mi-CK reacting with vesicles containing 16% CL. After each association/dissociation cycle, the avidin surface was washed with 1% SDS.

(RU), *k*<sub>1</sub> and *k*<sub>2</sub> the two rate constants (both in units of s<sup>−1</sup>), and *t* the time (s). Each of the exponential terms represents the separate time course of Mi-CK binding to one kind of binding site. Both reactions are assumed to occur independently, each following a first-order rate law. To avoid the influence of bulk refractive effects, the first 20 s after the injection of the protein were not taken into consideration. Therefore, the association rate constants *k*<sub>1</sub> (fast) and *k*<sub>2</sub> (slow) were determined by fitting the experimental curve in the time interval from 20 to 220 s after injection of Mi-CK. For immobilized PC vesicles containing 16% cardiolipin the fast association rate constant *k*<sub>1</sub> was found to be  $1.12 \times 10^{-1} \pm 7.98 \times 10^{-4}$  s<sup>−1</sup>, whereas the slower constant *k*<sub>2</sub> was determined to  $9.30 \times 10^{-3} \pm 6.88 \times 10^{-5}$  s<sup>−1</sup>. Interestingly, almost the same association rate constants were found for vesicles containing 100% cardiolipin where the value of *k*<sub>1</sub> was  $1.14 \times 10^{-1} \pm 1.34 \times 10^{-3}$  s<sup>−1</sup> and for *k*<sub>2</sub> a rate constant of  $7.6 \times 10^{-3} \pm 1.06 \times 10^{-4}$  s<sup>−1</sup> was determined. Figure 3 shows three representative examples of the measured association kinetics of octameric Mi-CK to vesicles containing 100% CL together with the best fits, demonstrating the close approximation of the fitted curves to the experimental data. The low standard errors of 1–2% for all association rate constants (see Table 1) further support the validity of the applied model. Transport limitation effects (Schuck & Minton, 1996) were excluded by the experimental design used (Figure 1).

The dissociation curves were fitted to the same model as described for the association reaction, i.e., a sum of exponential functions. In this case, the fit function was

$$y = (m_1 - m_2)e^{-k_{-1} t} + m_2 e^{-k_{-2} t} \quad (2)$$

with *m*<sub>1</sub> representing the initial response signal (RU) and *k*<sub>−1</sub> and *k*<sub>−2</sub> the two dissociation rate constants. The other variables have the same meaning as in eq 1. For similar

Table 1: Kinetic and Equilibrium Constants of the Mi-CK/Vesicle System

	cardiolipin content of vesicles	
	16%	100%
$k_1$ (fast association) ( $s^{-1}$ )	$1.12 \times 10^{-1} \pm 7.98 \times 10^{-4}$	$1.14 \times 10^{-1} \pm 1.34 \times 10^{-3}$
$k_2$ (slow association) ( $s^{-1}$ )	$9.30 \times 10^{-3} \pm 6.88 \times 10^{-5}$	$7.6 \times 10^{-3} \pm 1.06 \times 10^{-4}$
$k_{-1}$ (fast dissociation) ( $s^{-1}$ )	$1.64 \times 10^{-2} \pm 2.68 \times 10^{-4}$	$2.96 \times 10^{-2} \pm 4.64 \times 10^{-3}$
$k_{-2}$ (slow dissociation) ( $s^{-1}$ )	$3.26 \times 10^{-4} \pm 5.88 \times 10^{-6}$	$1.40 \times 10^{-4} \pm 2.34 \times 10^{-5}$
$K_1$ ( $k_1/k_{-2}$ ) (high-affinity) <sup>a</sup>	$343.6 \pm 3.7$	$813.7 \pm 126.5$
$K_2$ ( $k_2/k_{-1}$ ) (low-affinity) <sup>a</sup>	$5.7 \times 10^{-1} \pm 5 \times 10^{-3}$	$2.6 \times 10^{-1} \pm 3.7 \times 10^{-2}$
$k_3$ (cross-linking) ( $s^{-1}$ )	$6.25 \times 10^{-3} \pm 2.13 \times 10^{-4}$	$2.55 \times 10^{-3} \pm 1.65 \times 10^{-4}$

<sup>a</sup> The equilibrium constants are dimensionless because all the rate constants bear the units ( $s^{-1}$ ).

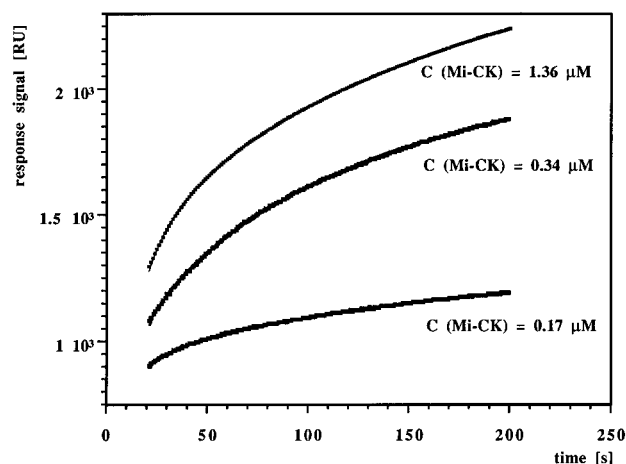


FIGURE 3: Kinetic fits of the association reaction of octameric Mi-CK measured with plasmon resonance (BiaCore). The association phases of three representative plots of different concentrations of octameric Mi-CK reacting with 600 RU of immobilized lipid vesicles (100% CL) are shown. The curves were fitted to a sum of two exponential functions using the program Kaleidagraph. Each time course shows a correlation of at least 99%.

reasons as described for the association kinetics (see above), the first 20 s after buffer injection were not taken into account to evaluate the best fits. For vesicles containing 16% CL, the measured curves were fitted to the time interval from 20 to 220 s after buffer injection. The two first-order dissociation constants differed by 2 orders of magnitude. The obtained constants were  $1.64 \times 10^{-2} \pm 2.68 \times 10^{-4} s^{-1}$  ( $k_{-1}$ , fast dissociation) and  $3.26 \times 10^{-4} \pm 5.88 \times 10^{-6} s^{-1}$  ( $k_{-2}$ , slow dissociation), respectively. Thus, both constants contain a standard error less than 2%. For Mi-CK bound to vesicles containing 100% CL, the dissociation rate constants were  $2.96 \times 10^{-2} \pm 4.64 \times 10^{-3} s^{-1}$  ( $k_{-1}$ ) and  $1.40 \times 10^{-4} \pm 2.34 \times 10^{-5} s^{-1}$  ( $k_{-2}$ ). In this case the standard error for both dissociation rate constants was much higher (about 16%) due to the smaller signal amplitude and the smaller time frame of 70 s (20–90 s after buffer injection) evaluated to get an optimum fit.

The determined rate constants allowed the calculation of the association equilibrium constants for the two kinds of binding sites. For both kinds of vesicles, the slow association and the fast dissociation produce a small signal amplitude. Therefore, the corresponding equilibrium constant  $K_2$  is given by  $k_2/k_{-1}$  and represents the low-affinity equilibrium. Accordingly, the high-affinity equilibrium constant  $K_1$  was calculated by  $k_1/k_{-2}$  because  $k_1$  (fast association) and  $k_{-2}$  (slow dissociation) contribute the major part to the total signal amplitude (Figure 2). The measured rate constants and the equilibrium constants are summarized in Table 1. Note that the equilibrium constant is dimensionless because both

the association and dissociation rate constants bear the same unit.

**Mi-CK-Induced Cross-Linking of Lipid Vesicles.** The vesicle cross-linking kinetics of octameric Mi-CK in free solution were investigated by light-scattering measurements in a fluorimeter. This technique already has been successfully used to examine histone aggregation (Smerdon & Isenberg, 1974) and binding of coagulation factors to vesicles (Cutsforth et al., 1989). In the system examined here, the addition of octameric Mi-CK to a vesicle suspension leads to a decrease of the light intensity at a detection angle of  $90^\circ$  which was indicative for Mi-CK-induced vesicle cross-linking (Figure 4). The reaction turned out to be almost irreversible even after diluting the Mi-CK/vesicle complex 10-fold. To avoid the extensive formation of higher aggregates, the vesicle concentration was kept in the subnanomolar range (0.24–0.8 nM) and the concentration range of Mi-CK was 17–28 nM. Under these conditions the cross-linking rate turned out to be independent of the vesicle concentration (data not shown). The scattering curves could be fitted to a one-exponential function

$$y = m_1 + (m_2 - m_1)e^{-k_3 t} \quad (3)$$

with  $m_1$  being the asymptotic value of the final signal intensity (counts per second, cps),  $m_2$  the initial intensity (cps), and  $k_3$  the cross-linking rate constant ( $s^{-1}$ ). To avoid mixing and local overconcentration effects, all scattering curves were fitted from 50 to 700 s after addition of the protein (Figure 4b). Interestingly, liposomes containing 16% CL gave rise to a faster  $k_3$  than vesicles containing exclusively CL. The pseudo-first-order rate constant  $k_3$  was  $6.25 \times 10^{-3} \pm 2.13 \times 10^{-4} s^{-1}$  (10 constants averaged) for liposomes with 16% CL and  $2.55 \times 10^{-3} \pm 1.65 \times 10^{-4} s^{-1}$  for liposomes containing 100% CL (10 constants averaged). It has to be pointed out that the relationship between the measured intensity and the number of aggregates formed is not linear due to overlapping scattering contributions from different intermediate species. Thus, the observed decrease of the scattering intensity reflects an average time course for the cross-linking reaction. As a consequence, the measured cross-linking constants have merely phenomenological significance. Nevertheless, our results clearly show that the binding of Mi-CK to vesicles (as determined in the BiaCore experiments) is much faster than the formation of the cross-linked complexes. These findings are best described by a model involving a fast binding equilibrium of Mi-CK to vesicles and a slow, rate-limiting step for the cross-linking reaction according to the following scheme:

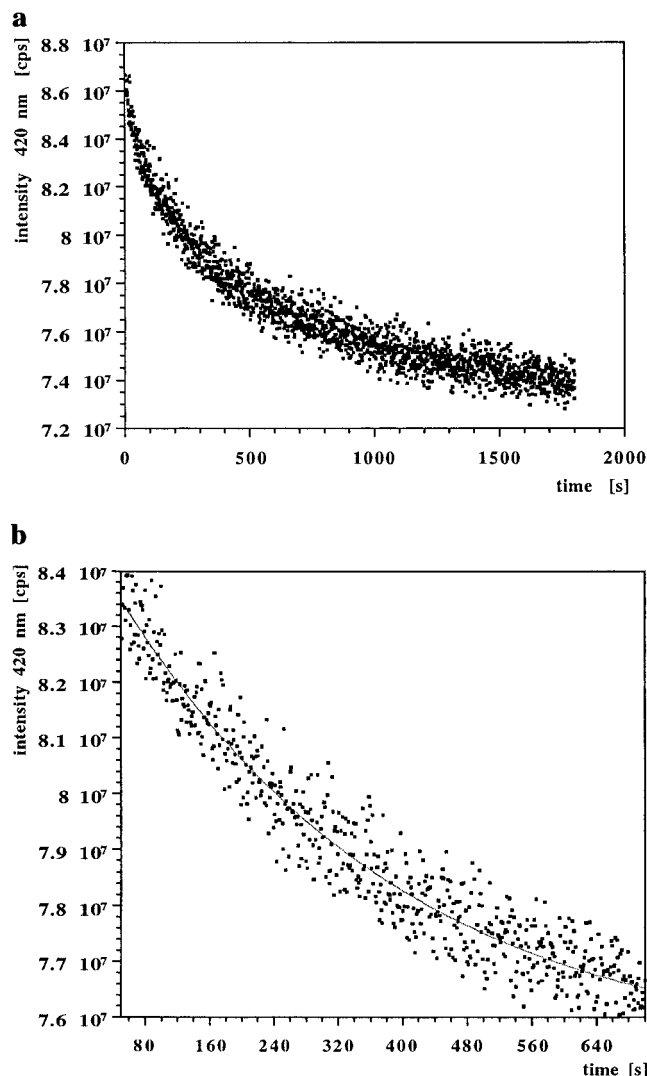
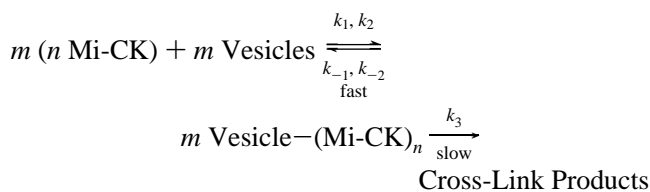


FIGURE 4: Cross-linking kinetics of octameric Mi-CK and vesicles containing 100% CL in free solution measured by light scattering. Time course of the Mi-CK-induced vesicle cross-linking measured at 420 nm wavelength (a). Vesicles ( $c = 350$  pM) were preincubated in reaction buffer; then Mi-CK was injected to give a final protein concentration of 20.4 nM. Finally, the measured curve was fitted to a one-exponential function from 50 to 700 s after injection of the protein (b).



As a control, the cross-linking experiment was carried out with dimeric Mi-CK (>95% dimer) under the same conditions as described for the octameric enzyme. In this case, no remarkable signal decrease was detected, i.e., under these conditions no cross-linking reaction occurred. However, dimeric Mi-CK was shown to bind to phospholipid vesicles (O. Stachowiak, M. Dolder, and T. Wallimann, unpublished results). A highly symmetrical arrangement of four dimers leading to an octamer with identical top and bottom face (Figure 5) is thought to be responsible for the observed difference in the membrane cross-linking capabilities between the Mi-CK dimer and octamer (Rojo et al., 1991a). Our findings strongly support the statement that it is the octameric

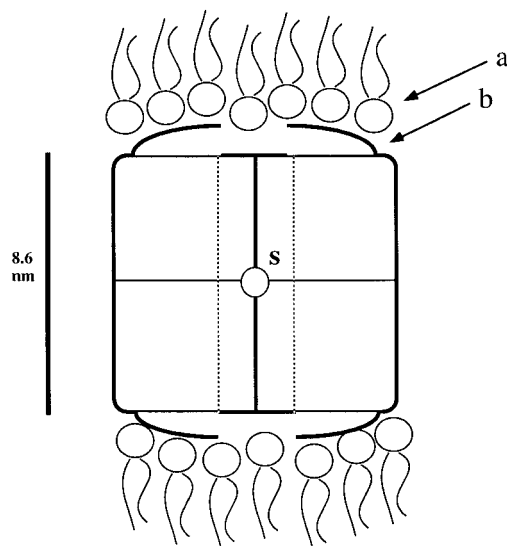


FIGURE 5: Schematic representation of octameric Mi-CK and its interaction with the mitochondrial membrane. Side view of octameric Mi-CK showing the possible interaction of membrane lipids (a) and Mi-CK via the four lysine- and arginine-rich C-termini (b) of the enzyme on the top and bottom face. The smaller side channel (S) is parallel to a two-fold symmetry axis, whereas the central main channel of 2 nm diameter (dashed lines) runs parallel to the fourfold symmetry axis ( $P422$  symmetry).

form of Mi-CK which is necessary to provide efficient membrane cross-linking.

## DISCUSSION

For the first time, data obtained by a quantitative kinetic approach using a well-defined *in vitro* model system which describes the vesicle-binding properties of octameric mitochondrial creatine kinase are presented. To establish reproducible conditions, vesicles with defined lipid compositions were prepared. With the BiaCore approach, difficulties associated with Mi-CK-induced vesicle aggregation were avoided and both association and dissociation rate constants could be measured with high reproducibility. Another advantage of this technique is that immobilized vesicles, in contrast to freely diffusible liposomes, present only part of their surface for protein binding, which is closer to the *in vivo* situation between the mitochondrial membranes.

Our results for the association/dissociation kinetics (see Table 1) are in accordance with the originally proposed model of vesicles containing two independent binding sites for Mi-CK. In addition, our data are in qualitative agreement with earlier findings for octameric Mi-CK binding to mitoplasts (Schlame & Augustin, 1985). Based on Scatchard plots, these authors report the existence of two binding sites for Mi-CK on mitoplasts with dissociation constants differing by about 2 orders of magnitude. Comparing our numerical values for the association equilibrium constants  $K_1$  and  $K_2$ , it is evident that the difference in the affinity of Mi-CK to these sites is enormous, justifying the notation of high- and low-affinity binding sites. The former contribute 66% in vesicles containing 16% CL and 84% in pure CL vesicles to the total amount of binding sites. These values were estimated from the relative signal amplitudes 200 s after buffer injection to Mi-CK-covered vesicles in the BiaCore. After this time, most of the tightly bound protein molecules are still bound on the vesicle surface, whereas those bound to the low-affinity sites have been completely removed.

Considering the low value of  $K_2$ , we conclude that binding of Mi-CK to these sites is merely a loose, unspecific association of Mi-CK octamers which are not properly oriented for specific, tight binding to the membrane.

As can be seen from Table 1, there is no striking difference in the association behavior of octameric Mi-CK to the high-affinity binding sites of vesicles containing 16% or 100% CL. In particular, a higher CL content resulting in more negative charges on the membrane surface does not accelerate the association reaction of Mi-CK. This indicates that the association is not dominated by ionic forces which are restricted to low distances in a medium with a high dielectric constant (the Debye length is about 1.5 nm in a 50 mM NaCl solution). In contrast, the CL content of the membrane greatly influences the dissociation reaction as can be seen by the faster dissociation rate constant  $k_{-2}$  for vesicles containing the lower amount of CL. As a consequence, Mi-CK is bound more tightly to vesicles containing 100% CL, resulting in a higher value of the high-affinity equilibrium constant  $K_1$ . Ionic interactions are likely to contribute to this effect due to the close distance of the positively charged C-termini of bound Mi-CK octamers to the negatively charged cardiolipin molecules. However, comparing the surface charge density of both kinds of vesicles, it is expected that the affinity of Mi-CK to vesicles with 16% CL would be 10 times less than to pure CL vesicles. From this we conclude that ionic interactions are not the only reason for Mi-CK binding to liposomes. From the dissociation data it can be seen that at the end of the dissociation phase 66% of Mi-CK remained bound to the vesicles containing 16% CL which represents the CL content of the inner mitochondrial membrane. Similar values for the amount of bound Mi-CK were found for isolated mitochondrial membranes (Rojo et al., 1991a) and for mitoplasts (Schlegel et al., 1988). On the other hand, pure CL vesicles retained about 84% of the bound protein. These values further support the role of cardiolipin for Mi-CK binding and are in good accordance with literature data proposing that CL is one of the most important receptors because of its high abundance in the inner mitochondrial membrane (Müller et al., 1985; Cheneval et al., 1989; Rojo et al., 1991a). The high value for the calculated association equilibrium constant  $K_1$  (343.6 for 16% CL vesicles) indicates that *in vivo* almost all of the octameric Mi-CK must be bound to the inner membrane. If we take into consideration that at an estimated CK concentration of 5–10 mg/mL between the mitochondrial membranes almost exclusively octamers are found (Gross et al., 1993; Gross, 1994), it can be concluded that *in vivo* there is only very little freely diffusing CK in the mitochondrial intermembrane space.

Based on the experimental fact that Mi-CK and the adenine nucleotide translocase (ANT) are functionally coupled (Jacobus, 1985; Saks et al., 1985, 1994), a direct interaction of Mi-CK with integral proteins of the inner membrane like the ANT has been postulated (Kottke et al., 1991; Brdiczka, 1991). The data presented in this work show that the binding of Mi-CK to pure lipid vesicles is so prevalent that there is no need for a high affinity of ANT to Mi-CK. The translocase is associated with several tightly bound cardiolipin molecules (Beyer & Klingenberg, 1985) which are important for structural integrity and activity of this carrier. Therefore, a putative physical interaction between Mi-CK

and ANT may be mediated by the negatively charged CL bound to the translocase.

Mi-CK has been found in mitochondrial contact sites together with ANT and porin (Brdiczka, 1991; Brdiczka et al., 1994). Therefore, we have quantitatively analyzed Mi-CK-induced vesicle cross-linking by light scattering. Under the experimental conditions used, only octameric Mi-CK was able to cross-link lipid vesicles, whereas dimeric Mi-CK failed to induce vesicle cross-linking for both kinds of liposomes. These data are confirmed by Lipskaya and Trofimova who argued that *in vivo* membrane cross-linking is only caused by the Mi-CK octamer (Lipskaya & Trofimova, 1989a). The lower potency of the dimer to cross-link membranes was also shown by experiments using lipid monolayers and vesicles (Rojo et al., 1991a,b). The measured scattering curves could not be fitted unequivocally with a model curve involving a defined reaction order. This may have to do with the complex time course and reaction mechanism of Mi-CK-induced vesicle cross-linking. The best fits were obtained by applying a first-order exponential function to the time interval from 50 to 700 s. This yielded a phenomenological first-order rate constant which can be used to compare the cross-linking kinetics with the association/dissociation data. The data show that vesicle cross-linking occurs slower by about 2 orders of magnitude than association of Mi-CK to the high-affinity binding sites. This indicates that cross-linking occurs between Mi-CK-covered vesicles. The cross-linking rate for vesicles containing 16% CL is more than 2 times faster than for pure CL vesicles. This cannot sufficiently be explained by the electrostatic repulsion of vesicles containing 100% CL as the Debye length is too short (1.5 nm, see above) compared with the dimension of octameric Mi-CK (~10 nm). Cross-linking of vesicles probably requires a certain conformational and/or rotational flexibility of membrane-bound Mi-CK. As the protein binds more tightly to 100% CL vesicles, it may be restricted in its mobility, which would partially explain the slower cross-linking rate observed for pure CL vesicles.

The quantitative *in vitro* data presented here are in agreement with the high-resolution X-ray structure of the Mi-CK octamer (Fritz-Wolf et al., 1996), showing four lysine- and arginine-rich C-termini exposed on both surfaces. These residues are most likely involved in membrane binding and noncovalent cross-linking of vesicles. The data also support the hypothesis of octameric Mi-CK being involved in the formation of mitochondrial energy-channeling contact sites (Schnyder et al., 1994; Wallimann et al., 1992; Wyss et al., 1992; Wyss & Wallimann, 1992). In addition, the membrane-linking properties and the association behavior of octameric Mi-CK shown to form crystalline intramitochondrial inclusions between the inner and outer membrane and between cristae membranes in patients with mitochondrial cytopathies (Stadhouders et al., 1994), in cardiomyocytes cultured in the absence of creatine (Eppenberger-Eberhardt et al., 1991), or in rats made deficient in creatine (O'Gorman et al., 1996) are corroborated by our biophysical data. Therefore, an accumulation of Mi-CK along the mitochondrial membranes caused by the high affinity of the enzyme to the latter is likely to be a crucial factor responsible for the formation of crystalline aggregates seen in mitochondria under metabolic energy stress.

In conclusion, the techniques presented in this work should allow to quantitate interactions between Mi-CK and recon-

stituted membrane proteins like ANT and porin. Corresponding experiments are currently in progress to elucidate the role of these integral membrane proteins in Mi-CK membrane binding and cross-linking. From these measurements we expect detailed information about the origin and nature of mitochondrial contact-site formation.

## ACKNOWLEDGMENT

Prof. R. Glockshuber, Prof. M. Smerdon, Dr. P. Schurtenberger, and Prof. D. Brdiczka are kindly acknowledged for many fruitful discussions. We are indebted to Dr. G. Orberger for constant support at the BiaCore system.

## REFERENCES

- Bartlett, G. R. J. (1959) *J. Biol. Chem.* **234**, 466.
- Beyer, K., & Klingenberg, M. (1985) *Biochemistry* **24**, 3821–3826.
- Bradford, M. M. (1976) *Anal. Biochem.* **72**, 248–254.
- Brdiczka, D. (1991) *Biochim. Biophys. Acta* **1071**, 291–312.
- Brdiczka, D., Kaldis, P., & Wallimann, T. (1994) *J. Biol. Chem.* **269**, 27640–27644.
- Cheneval, D., Carafoli, E., Powell, G. L., & Marsh, D. (1989) *Eur. J. Biochem.* **186**, 415–419.
- Cutsforth, G. A., Whitaker, R. N., Hermans, J., & Lentz, B. (1989) *Biochemistry* **28**, 7453–7461.
- Eppenberger, H. M., Perriard, J. C., & Wallimann, T. (1983) *Curr. Top. Biol. Med. Res.* **7**, 19–38.
- Eppenberger-Eberhardt, M., Riesinger, J., Messerli, M., Schwarb, P., Müller, M., Eppenberger, H. M., & Wallimann, T. (1991) *J. Cell Biol.* **113**, 289–302.
- Fritz-Wolf, K., Schnyder, T., Wallimann, T., & Kabsch, W. (1996) *Nature* **381**, 341–345.
- Gross, M. (1994) Ph.D. Thesis, No. 10719, Swiss Federal Institute of Technology, Zürich.
- Gross, M., & Wallimann, T. (1993) *Biochemistry* **32**, 13933–13940.
- Jacobus, W. E. (1985) *Annu. Rev. Physiol.* **47**, 707–725.
- Johnsson, B., Löfas, S., & Lindquist, G. (1991) *Anal. Biochem.* **198**, 268–277.
- Kottke, M., Adams, V., Wallimann, T., Kumar Nalam, V., & Brdiczka, D. (1991) *Biochim. Biophys. Acta* **1061**, 215–225.
- Lipskaya, T. Yu., & Trofimova, M. E. (1989a) *Biochem. Int.* **18**, 1129–1139.
- Lipskaya, T. Yu., & Trofimova, M. E. (1989b) *Biochem. Int.* **18**, 1149–1159.
- MacDonald, R. C., MacDonald, R., Menco, B. Ph. M., Takeshita, K., Subbarao, N. K., & Hu, L. (1991) *Biochim. Biophys. Acta* **1061**, 297–303.
- Marcillat, O., Goldschmidt, D., Eichenberger, D., & Vial, C. (1987) *Biochim. Biophys. Acta* **890**, 233–241.
- Masson, L., Mazza, A., & Brousseau, R. (1994) *Anal. Biochem.* **218**, 405–412.
- Müller, M., Moser, R., Cheneval, D., & Carafoli, E. (1985) *J. Biol. Chem.* **260**, 3839–3843.
- O'Gorman, E., Beutner, G., Wallimann, T., & Brdiczka, D. (1996) *Biochim. Biophys. Acta* **1276**, 161–170.
- Rojo, M., Hovius, R., Demel, R. A., Wallimann, T., Eppenberger, H. M., & Nicolay, K. (1991a) *FEBS Lett.* **281**, 123–129.
- Rojo, M., Hovius, R., Demel, R. A., Nicolay, K., & Wallimann, T. (1991b) *J. Biol. Chem.* **266**, 20290–20295.
- Saks, V. A., Khuchua, Z. A., Vasilyeva, E. V., Belikova, O. Yu., & Kusnetzov, A. V. (1994) *Mol. Cell. Biochem.* **133/134**, 155–193.
- Schlame, M., & Augustin, W. (1985) *Biomed. Biochim. Acta* **44**, 1083–1088.
- Schlegel, J., Wyss, M., Schürch, U., Schnyder, T., Quest, A., Wegmann, G., Eppenberger, H. M., & Wallimann, T. (1988) *J. Biol. Chem.* **263**, 16963–16969.
- Schlegel, J., Wyss, M., Eppenberger, H. M., & Wallimann, T. (1990) *J. Biol. Chem.* **265**, 9221–9227.
- Schnyder, T., Winkler, H., Gross, H., Eppenberger, H. M., & Wallimann, T. (1991) *J. Biol. Chem.* **266**, 5318–5322.
- Schnyder, T., Rojo, M., Furter, R., & Wallimann, T. (1994) *Mol. Cell Biochem.* **133/134**, 115–123.
- Schuck, P., & Minton, A. P. (1996) *Anal. Biochem.* **240**, 262–272.
- Smerdon, M. J., & Isenberg, I. (1973) *Biochem. Biophys. Res. Commun.* **55**, 1029.
- Stadhouders, A. M., Jap, P., Winkler, H. P., Eppenberger, H. M., & Wallimann, T. (1994) *Proc. Natl. Acad. Sci. U.S.A.* **91**, 5089–5094.
- Vial, C., Font, B., Goldschmidt, D., & Gautheron, D. C. (1983) *Arch. Biochem. Biophys.* **220**, 541–548.
- Wallimann, T. (1994) *Curr. Biol.* **4**, 42–46.
- Wallimann, T., Schlösser, T., & Eppenberger, H. M. (1984) *J. Biol. Chem.* **259**, 5238–5246.
- Wallimann, T., Wyss, M., Brdiczka, D., Nicolay, K., & Eppenberger, H. M. (1992) *Biochem. J.* **281**, 21–40.
- Wegmann, G., Huber, R., Zanolla, E., Eppenberger, H. M., & Wallimann, T. (1991) *Differentiation* **46**, 77–87.
- Wyss, M., & Wallimann, T. (1992) *J. Theor. Biol.* **158**, 129–132.
- Wyss, M., Smeitink, J., Wevers, R. A., & Wallimann, T. (1992) *Biochim. Biophys. Acta* **1102**, 119–166.

BI961838V